

A roadmap for searching cosmic rays correlated with the extraterrestrial neutrinos seen at IceCube

J.A. Carpio and A.M. Gago

Sección Física, Departamento de Ciencias, Pontificia Universidad Católica del Perú, Apartado 1761, Lima, Perú

We have built Sky maps showing the expected arrival directions of 120 EeV ultrahigh energy cosmic rays (UHECR) directionally correlated with the latest astrophysical neutrino tracks observed at IceCube, including the 4-year high-energy starting events (HESE) and the 2-year Northern tracks, taken as point sources. We have considered contributions to UHECR deflections from the galactic and the extragalactic magnetic field, and a UHECR composition compatible with the current expectations. We have used the Jansson-Farrar JF12 model for the Galactic magnetic field and an extragalactic magnetic field strength of 1nG and coherence length of 1Mpc. We observe that the regions outside of the Galactic plane are more strongly correlated with the neutrino tracks than those adjacent to or in it, where IceCube HESE events 37 and 47 and, from the 2-year Northern hemisphere sample, event *N*13 are good candidates to search for excesses, or anisotropies, in the UHECR flux. On the other hand, clustered Northern tracks around $(l, b) = (0^\circ, -30^\circ)$ are promising candidates for a stacked point source search. As an example, we have focused on the region of 150 EeV UHECR arrival directions correlated with IceCube HESE event 37 located at $(l, b) = (-137.1^\circ, 65.8^\circ)$ in the Northern Hemisphere, far away from the Galactic plane, obtaining an angular size $\sim 5^\circ$, being $\sim 3^\circ$ for 200 EeV, and $\sim 8^\circ$ for 120 EeV.

I. INTRODUCTION

The discovery of extraterrestrial neutrinos made by the IceCube (IC) Neutrino Observatory [1–3] has boosted the multimessenger searches of point sources, which eventual results should lead us to understand the high-energy astrophysical phenomena. Within this context, it is believed that extraterrestrial neutrinos are created inside or outside the source, primarily through photopion production. The pion production is caused by the interaction of ultrahigh energy cosmic rays (UHECR) either with the cosmic microwave background (CMB) or with the extragalactic background light (EBL) [4], yielding neutrinos from their decay, with energies in the range of 10PeV-1EeV or in $\mathcal{O}(\text{PeV})$, respectively. Thus, given the connection between UHECR and neutrinos, some degree of correlation between their respective experimental observations is expected. This kind of study has been already conducted using the extraterrestrial neutrinos observed at IceCube and a combined UHECR data from the Pierre Auger Observatory (PAO) and Telescope Array (TA), with not a positive outcome yet [5]. There have also been other attempts to seek correlations between photons and neutrinos [6] or gravitational waves with neutrinos [7]. In the future, multimessenger searches, such as joint neutrino/gamma-ray transient sources, will be facilitated by AMON [8].

The correlation analysis between UHECRs and neutrinos, as has been done in [5], relies on the distribution of cosmic ray arrival directions. This paper uses another approach to this issue. In our case, we will focus on predicting the regions on the Sky where UHECRs correlated with neutrinos are expected to arrive, considering that the neutrino tracks are pointing to the sources. In this way, these regions will constitute a tool for searching UHECR excesses on the Sky. Besides, searches in these regions could be used as complementary test of the

various hypothesis implied in their construction, among others, the magnetic field model, the UHECR composition and, at a more fundamental level, the expected associated production of UHECR and neutrinos.

In fact, the choice of the Galactic and extragalactic magnetic field model is one of the most important hypothesis in our work. These fields deviate the UHECRs from its path to the Earth, making their arrival directions to not coincide with the corresponding ones of the neutrinos. For the extragalactic magnetic field (EGMF), we will use a turbulent field of strengths $\sim 1\text{nG}$ and coherence lengths $\gtrsim 1\text{Mpc}$ following the references [9, 10]. For the Galactic magnetic field (GMF), we will use field strengths of $\sim 1\mu\text{G}$. The GMF is divided into a regular and a turbulent component, the former described by models such as those in [11, 12] and the latter in [13]. The GMF deflections are dominated by the regular components, to which is added, as a secondary effect, a smearing due to the turbulent component. Another premise in the calculation of the magnetic deviation is the UHECR mass composition, which is taken into account in this paper, as it is described in sections ahead. Currently, the PAO has yet to explore the mass composition above 50 EeV, although a trend towards a heavy composition above 10 EeV is apparent [14, 15]. We select 13 muons tracks from the extraterrestrial neutrino data sample given by IceCube in the 79-string and 86-string configurations [1–3], which spans the deposited energy range 60TeV-1PeV. This is equivalent to four years of data taking and gives us an $E_\nu^{-2.58}$ neutrino flux spectrum and a flux of $2.2 \pm 0.7 \times 10^{-18} \text{ GeV}^{-1} \text{ cm}^{-2} \text{ s}^{-1} \text{ sr}^{-1}$ at 100 TeV. We choose 21 muon neutrino tracks from the two-year sample [16], consisting of tracks coming from the Northern Hemisphere, containing approximately 35000 muon tracks. A subsample of the 21 tracks with the highest energies was released and are likely to be of astrophysical origin. [?]

The paper is divided as follows: in section II we describe the analysis ingredients, which are: the extragalactic magnetic field deflections with its corresponding treatment for UHECR propagation, the galactic magnetic field deflection and the definitions for signal and background. In section III we present our results and, finally, in section IV our conclusions.

II. ANALYSIS INGREDIENTS

We subdivided this section into three parts: the EGMF deflections and UHECR propagation, GMF deflections and the Signal and Background definitions.

A. EGMF Deflections and UHECR propagation

Typical deflections in a turbulent EGMF with a Kolmogorov spectrum are given by [10]

$$\delta_{\text{rms}} = 0.8^\circ Z \left(\frac{B_0}{E} \frac{10^{20}\text{eV}}{10^{-9}\text{G}} \right) \sqrt{\frac{D}{10\text{Mpc}}} \sqrt{\frac{L_c}{1\text{Mpc}}}, \quad (1)$$

where B_0 is the EGMF root-mean-square field strength, E is the UHECR energy, L_c the coherence length of the field and D is the propagation distance, which starts from the UHECR. There is no general consensus on the values of B_0 and L_c [9, 10], in particular, we are using the values of 1 nG and 1 Mpc, respectively. Due to the large propagation distances of order > 10 Mpc, energy losses are taken into account being obtained from forward tracking via Monte Carlo simulation using CRPropa 3[17]. These energy loss processes include: cosmological expansion, photopion production and photodisintegration. For the latter two processes provide both the CMB and the infrared background light (IBL) described in [18].

We estimate the magnetic deflections through the injection of individual events from the following spectrum [19]

$$Q_Z(E_p) \propto \frac{E_p^{-\gamma}}{\cosh[E_p/(ZR_{\text{max}})]}, \quad (2)$$

where E_p stands for primary UHECR energy and $R_{\text{max}} = 20$ EV marks the rigidity cutoff, where rigidity is defined, in general, as $R = E/(Ze)$. The sources emit p,He,N,Si,Fe nuclei [19] according to the following ratios

$$\text{p:He:N:Si:Fe} = 0.1 : 0.27 : 0.30 : 0.32 : 0.005 \quad (3)$$

and we assume a homogenous distribution of identical sources. The composition in Equation (3) fits well the Auger data reasonably and gives us a maximum distance of ~ 200 Mpc from which UHECR above 100EeV may reach the Earth. The propagation distance D decreases exponentially with the UHECR arrival energy E .

We then generate 10^6 Monte Carlo events, calculating the magnetic deflection with Equation (1) for small steps

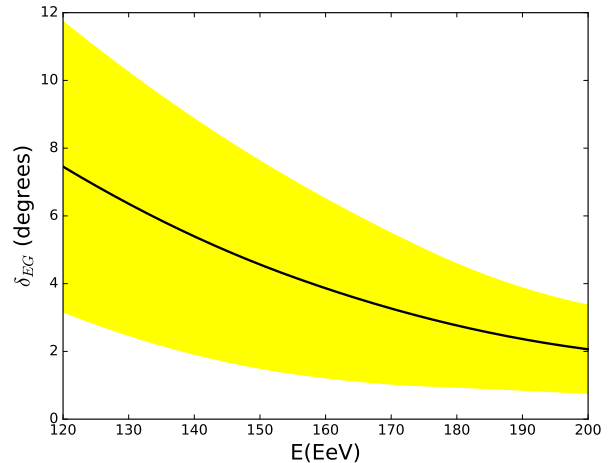


FIG. 1. δ_{EG} as a function of its arrival energy.

ΔL , due to the energy losses, adding them in quadrature. This amounts to the substitution

$$\frac{Z}{E} \sqrt{D} \rightarrow \sqrt{\sum_{i=1}^N \frac{Z^2(L)}{E^2(L)} \Delta L}, \quad (4)$$

where $N\Delta L = D$. These magnetic deflections also increase the UHECR propagation length by $\Delta D = \sum_{i=1}^N \Delta r$ where

$$\Delta r \simeq 0.195\text{Mpc} \frac{Z^2}{(E/\text{EeV})^2} \frac{L_c}{1\text{Mpc}} \left(\frac{\Delta L}{1\text{Mpc}} \right)^2. \quad (5)$$

Therefore, we obtain the deflections using (1) and (4) for a distance D , we let the particle propagate an additional ΔD , to see if the particle loses any extra energy. We use the latter approach, looking at extra energy losses, because $\Delta D \ll D$ and does not significantly contribute to the deflection

Finally, once the particle enters the Galaxy with an arrival energy E , we assign a deflection δ_{EG} per energy bin of width ΔE via

$$\delta_{EG}(E) = \text{Average } \delta_{\text{rms}} \text{ in bin}, \quad (6)$$

where $E \in [E_i, E_i + \Delta E]$. In figure 1, we display the values of δ_{EG} as a function of E . A band $[\delta_{EG} - \omega, \delta_{EG} + \omega]$ is included, such that 68% of the events in the bin are enclosed in this interval. Where we start with deflections intervals ranging between $[3^\circ, 12^\circ]$ at 120 EeV until reach deflections intervals, as small as $[1^\circ, 3^\circ]$ at 200 EeV.

B. GMF deflections

Once the cosmic ray enters the Galaxy with an energy E , we can ignore energy loss processes due to the relatively small size of the Galaxy ~ 40 kpc and trajectory

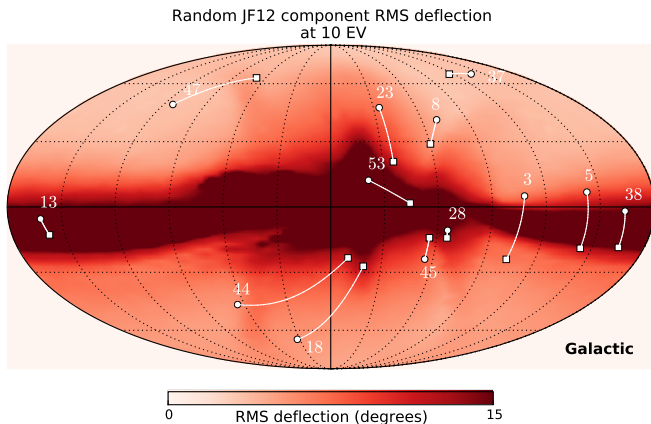


FIG. 2. RMS deflection of cosmic rays with rigidity 10EV. The white circles correspond to the reconstructed directions of HESE neutrino tracks and the white squares mark the expected arrival direction assuming only the JF12 coherent field. The white lines joining both are to match UHECRs with their corresponding track, they do not show the actual trajectory taken by the particle. Tracks are labeled by event numbers given in [3].

lengths < 100 kpc. Thus, the UHECR arrival energy at Earth is also E and the Galactic magnetic deflections will depend on the rigidity $R = E/(Ze)$.

We use the JF12 GMF model [11, 13], which is designed to fit the WMAP7 Galactic synchrotron emission map and more than 40,000 extragalactic Faraday rotation measurements. It is divided into three components: regular (coherent), striated (anisotropic) and an isotropic random field. The latter two are small-scale fields and will be referred to as the random or non-coherent components. We use the best fit values in [11], for the coherent field parameters, and in [13], for the random field parameters. The small scale field is assumed to have a coherence length of 60 pc.

We use the backtracking method to determine GMF deflections. For a hypothetical cosmic ray arriving at Earth, we reverse its incoming momentum vector, then change the sign of its charge. We propagate this particle from the Earth, through the GMF, until it leaves the Galaxy. The backtracking is performed using the Runge-Kutta methods in CRPropa 3.

We treat the GMF coherent and turbulent components separately, taking advantage of the JF12 Field parametrization outlined in [20]. Firstly, for a given initial direction $P_0 = (l_0, b_0)$ of a UHECR with energy E , where (l, b) are in the galactic coordinate system with $-180^\circ \leq l < 180^\circ$ the galactic longitude and $-90^\circ \leq b \leq 90^\circ$ the galactic latitude, we backtrack it through the coherent field to the position $P_c = (l_c, b_c)$. Starting from P_c , we perform an additional non-coherent field deflection, given by the von Mises-Fisher distribu-

tion [21]

$$f(\delta) = \frac{\kappa}{e^\kappa - e^{-\kappa}} \exp(\kappa \cos \delta), \quad (7)$$

where $\kappa = \kappa(l_0, b_0, R)$ is a fit parameter and δ is the angular distance between P_c and the final position of the particle. We also assume that the azimuthal distribution of this random deflection is flat. Contrary to the parametrization in [20], we were forced to extend the Rayleigh distribution to a von Mises-Fisher distribution in order to handle deflections that are not so small. This is caused by the low rigidity particles. The energy dependence in κ is given by

$$\kappa(l_0, b_0, R) = A_1(l_0, b_0)R + A_2(l_0, b_0)R^2. \quad (8)$$

This approximation has been tested in the rigidity range $10\text{EV} \leq R \leq 100\text{EV}$. The parameters A_1, A_2 were obtained using HEALPix [22] to divide the sky into 3072 pixels of equal solid angle. We emphasize that in the vicinity of the Galactic plane, where large deflections are present provided by the high turbulent fields components, the parametrization given in Equation (8) is unreliable and we solve these cases numerically.

In the small deflection hypothesis (valid for $< 15^\circ$), where $\kappa \gg 1$, concentration parameter κ is related to the root-mean-square deflection

$$\delta_{\text{Gal}} = \frac{1}{\sqrt{\kappa}}. \quad (9)$$

We assume an average rigidity $\langle R \rangle_E$ for all particles with a given energy E , which obeys the relation $\langle R \rangle_E \approx (E/10.5\text{EeV})\text{EV}$ according to our simulations.

The root-mean-square deflections at $R = 10$ EV for different arrival directions are shown in figure 2. We see that trajectories close to the Galactic center and/or plane can be affected by high ($> 15^\circ$) non-coherent deflections which exceed the angular resolution of experiments ($\sim 2^\circ$) by an order of magnitude. As a reference, we have included the reconstructed arrival directions of the high-energy starting events (HESE) neutrino tracks, labeled according to their corresponding event numbers as presented in [3]. We also marked the respective arrival directions of 10 EV UHECR, considering the aforementioned tracks as point source and ignoring EGMFs and the JF12 random field components.

C. Signal and Background

We work in a similar scenario such as described in [5], where a sample of N_{CR} UHECR and N_ν neutrinos is given. The neutrinos are considered as point sources, while the N_{CR} cosmic rays are a combination of signal and background events. We define \mathcal{S}_i^j as the probability density (pdf) that the i th cosmic ray came from the direction of the j th neutrino event.

$$\mathcal{S}_i^j = \frac{\kappa_i}{2\pi(e^{\kappa_i} - e^{-\kappa_i})} \exp(\kappa_i \mathbf{x}_i \cdot \mathbf{x}_j), \quad (10)$$

where $\kappa_i = 1/\sigma_i^2$ and σ_i accounts for the overall smearing of the i th cosmic ray. In the limit of small smearings \mathcal{S}_i^j reduces to a two-dimensional Gaussian. For single source searches, when $N_\nu = 1$, the signal pdf is $\mathcal{S}_i \equiv \mathcal{S}_i^1$ and is used in the unbinned likelihood analysis like the mentioned in [23]. For the so-called stacked source searches, when $N_\nu > 1$, we add up the contributions from multiple faint sources and the signal pdf is modified to

$$\mathcal{S}_i = \frac{1}{N_\nu} \sum_{j=1}^{N_\nu} \mathcal{S}_i^j. \quad (11)$$

In order to use any of these formulas, we substitute the arrival direction \mathbf{x}_i of the UHECR by its backtracked direction \mathbf{x}'_i , assuming that the only magnetic field involved is the regular JF12 component and that the particle's rigidity is given by $\langle R \rangle_E$. We then determine the values of κ_i and δ_{Gal} via Equations (8), that parametrizes the smearing effect of the non-regular component, and (9), respectively, which are functions of the UHECR energy and its arrival direction. The EGMF deflections and angular resolution effects are incorporated by making the substitution

$$\kappa_i \longrightarrow \frac{1}{\sqrt{\delta_{\text{Gal}}^2 + \delta_{EG}^2 + \delta_{\text{res}}^2}}, \quad (12)$$

with $\delta_{\text{Gal}} = \delta_{\text{Gal}}(\langle R \rangle_E)$, $\delta_{EG} = \delta_{EG}(E)$ and δ_{res} is the angular resolution of the experiment. We will assume an energy independent deflection $\delta_{\text{res}} = 2^\circ$ as a characteristic angular resolution for IceCube and UHECR ground array experiments.

For the large GMF deflections present at the Galactic plane, where Equation (8) is not valid, \mathcal{S}_i is determined entirely via Monte Carlo. We also define \mathcal{B}_i as the probability density that the CR is a background event. Typically $\mathcal{B}_i = 1/4\pi$ or, in the case of the analysis in [5], the normalized exposure of the experiment.

III. RESULTS

Now, we quantify how likely an observed UHECR, with a given arrival direction \mathbf{x}_i and energy E_i , could have the same origin as the neutrino track, which we treat as the UHECR point source, through the following ratio:

$$W_i = \frac{\int \mathcal{S}_i d\Omega}{\int \mathcal{B}_i d\Omega}, \quad (13)$$

where $d\Omega$ is integrated in a region of 1° in the Sky, centered around the neutrino track.

In figure 3, we show the effect of W_i in a single point source search, located at IC event 37 (l, b) = $(-137.1^\circ, 65.8^\circ)$ in the Northern hemisphere, labeled according to the numbering in Reference [5], in two plots. One is a two-dimensional map in the coordinates (l, b), where P_c marks the expected UHECR arrival direction, when considering only the JF12 coherent component.

The other one is its corresponding one-dimensional projection in angular distance centered in P_c , where the solid line is the average value of W_i and the shaded region covers the whole set of values given by the points at the angular distance contour. We have selected IC event 37 because it belongs to a region where the GMF random component deflections are very small, as shown in figure 2, being the random EGMF responsible for most of the smearing around P_c , displayed in the two-dimensional plot. These characteristics turn IC event 37 into a good candidate for searches of UHECR excesses around it. In both plots it is clear that P_c gives the highest ratio, since, by construction, it is here where the signal pdf is maximized. Ellipsoidal(vertical) solid/dashed lines are shown for the two(one) dimensional plot. The solid line represents the size of the typical or average angular search region $\delta_s = \sqrt{\delta_{\text{Gal}}^2 + \delta_{EG}^2 + \delta_{\text{res}}^2}$, measured from P_c , while the dashed lines include the effects of the spread in δ_{EG} shown in figure 1. Our results show that UHECRs confined within the region of size δ_s , that have the appropriate energy and arrival direction, would have very high values of W_i . In the one-dimensional plot, a band enclosing the W_i average is also displayed, and is caused by the anisotropy of the random deflections, or, equivalently, the B field itself. Otherwise, if the random deflections were isotropic, there would be no band, which means that all the values would converge to a single one. For small angular distances, the variation, or width of the band, of W_i , is small because the parameter κ_i is essentially constant, and as we move away from P_c this variation is significant.

For a wider perspective, we are showing in figure 4 the dependence of δ_s with UHECR arrival energy. It follows the same behaviour of δ_{EG} (see figure 1) since δ_s in the case of IC event 37 is dominated by the extragalactic contribution.

It is important to mention that in case the current or future ground array experiments were able to identify the UHECR mass, we would have a sensible improvement in our analysis since the uncertainties in the rigidity (i.e. δ_{EG}) are going to be small and inside the Galaxy we would know with greater precision the backtrack trajectory because R is constant within the Galaxy. The analysis is also dependent on the UHECR-neutrino sources being within the GZK sphere, such that we may observe the cosmic rays.

The sky map of W_i for a stacked search of cosmic ray events by using the IceCube tracks as the assumed point sources is presented in figure 5, which assumes incoming 120EeV cosmic rays, which is our lower energy limit in our analysis, and unknown mass number. This figure contains two Sky maps, one for the IC HESE event sample [5] and another for the combined sample of HESE events and the second one using both the 4-year HESE tracks and the 2-year IceCube Northern Sky tracks[16] in a combined search. As before, the circles represent the positions of the neutrino tracks. In the HESE Sky map, we also included squares indicating their respec-

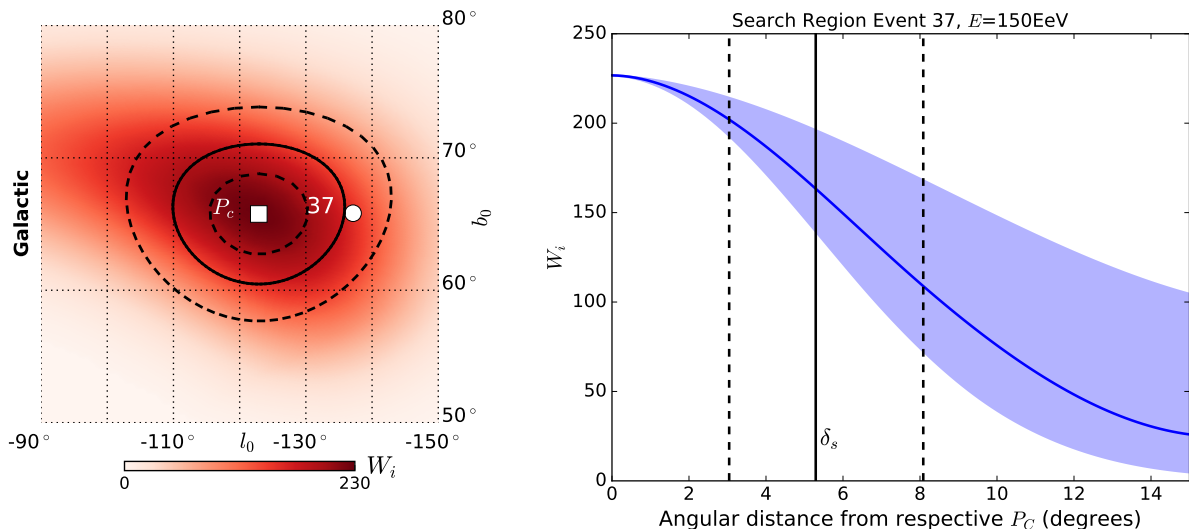


FIG. 3. W_i for a single point source search located at Event 37 and 150EeV UHECR. At the left we have the corresponding two-dimensional plot of W_i in the coordinates l_0 and b_0 . At the right we have the one-dimensional projection of W_i in the angular distance respect to P_c

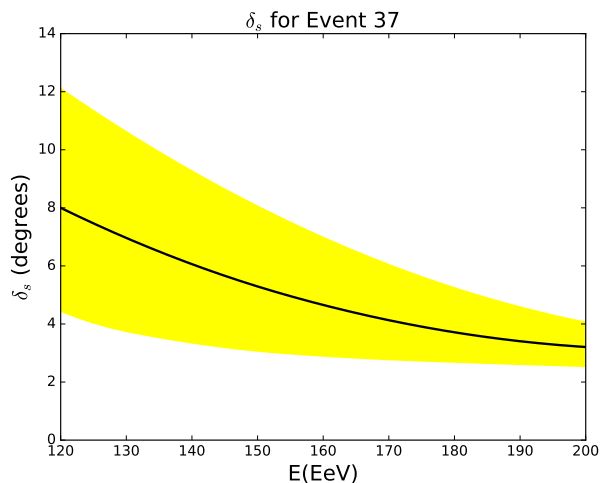


FIG. 4. δ_s angular size region for the IC event 37 as a function of UHECR arrival energy

tive points P_c when the neutrino tracks are close to each other. Here we observe that for events close to the Galactic plane, we do not have a well-defined region to correlate with the neutrino track. Instead, we have disjoint regions, above and below the Galactic plane, which represent similar low values of W_i , such as those in neutrino events 3, 5 and 38. This is caused by the large random component deflections in these regions, as we have seen in figure 2. There are out-of-plane events, such as events 8 and 23, 18 and 44, 28 and 45, which exhibit well-defined regions, but with the drawback that they may overlap with each other. Despite our inability to disentangle the point source of origin, these zones are interesting to look

for UHECR excesses, because the effect of GMF deflections is significantly reduced and obtain higher values of W_i . The ideal case for correlating UHECR with these neutrino tracks are the events 37 and 47, which are far away from the Galactic plane.

In the combined Sky map, we increase the number of regions where we can expect the arrival of UHECRs. However, due to the nature of the stacked search, which includes a $1/N_\nu$ factor in Equation (11), the W_i of well-spread tracks is flattened to very low values (see for example events 8 and 47). Meanwhile, when we have clustered tracks, the W_i are strongly enhanced, as we can see in the region close to $(l, b) = (0^\circ, -30^\circ)$. Even when using the enlarged sample, the suggested search region for HESE event 37 does not overlap with the others. It is interesting to highlight that the Northern event N13 exhibits a region with very large values of W_i , becoming a suitable candidate to be included in a point source search.

IV. SUMMARY AND CONCLUSIONS

We have built two Sky maps showing different regions where 120 EeV UHECR excesses with respect to the isotropic background should appear: one for the IC 4-year HESE tracks and another for a combined search using the 4-year HESE events and the 2-year Northern Sky tracks. These excesses are inferred from the measurement of the correlation between a given UHECR arrival direction with the IceCube neutrino tracks, which are taken as point sources. The GMF and EGMF deflections have been calculated, using, correspondingly, the JF12 model and EGMF of strength $\sim 1\text{nG}$ and coherence lengths $\gtrsim 1\text{Mpc}$. We note that the out-of-plane

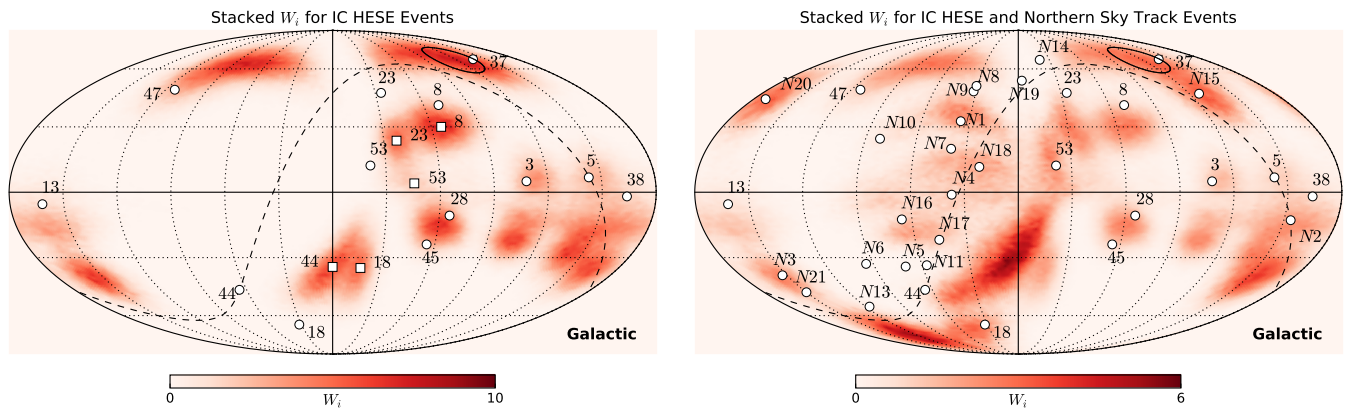


FIG. 5. Sky map for 120 EeV cosmic ray events of undetermined mass, using the 4-year IC HESE events (left panel) and a combined sample of IC HESE events and the 2-year IC Northern tracks (right panel). The white circles mark the neutrino tracks: HESE tracks are labeled according to their event numbers in [3]; Northern tracks, preceded by the letter N, are numbered according to the order in which they appear in the IceCube Data Release. The white squares mark the respective P_c of the track. Event N12 is not included in the map because it coincides with HESE track 5. The black dashed line marks the Equatorial plane. Suggested search region for event 37 is marked with a solid black line.

regions concentrate higher correlation values, quantified by the probability ratio W_i , being more promising than the ones near the Galactic plane for revealing excesses. Some of these regions can be correlated clearly with a single neutrino track, for instance in events 37, 47 and N13. These events are candidates to include in a point source search. For the stacked source search, good candidates include the tracks that contribute to the region in $(l, b) = (0^\circ, -30^\circ)$.

In particular, we take a closer look into event 37, where the GMF random component is negligible, considering an energy of 150 EeV and getting a region, where most of the UHECR excess should be located, of angular size $\sim 5^\circ$. If the UHECRs had energies of 120 EeV or 200 EeV the angular size would be $\sim 8^\circ$ or $\sim 3^\circ$, respectively. This similar tendency can be extrapolated to the Sky map where we expect regions with a much smaller angular spread, as long as we increase the UHECR energy. It is clear that the Sky map presented relies on the current statis-

tic of the neutrino tracks and as new data is released, we may obtain more favourable search regions. Naturally, the possibility to find UHECR in these regions intrinsically depends on these sources being located within the GZK sphere. Finally, we must say that the results of this analysis should improve if the ground array experiments identify the UHECR mass.

ACKNOWLEDGMENTS

The authors gratefully acknowledge DGI-PUCP for financial support under Grant No. 2014-0064, as well as CONCYTEC for graduate fellowship under Grant No. 012-2013-FONDECYT. The authors also want to thank Mauricio Bustamante and José Bellido for useful suggestions.

-
- [1] M.G. Aartsen et al. (IceCube Collaboration), *Evidence for High-Energy Extraterrestrial Neutrinos at the IceCube Detector*, Science **342** (2013) 1242856 [astro-ph/1311.5238].
 - [2] M.G. Aartsen et al. (IceCube Collaboration), *Observation of High-Energy Astrophysical Neutrinos in Three Years of IceCube Data*, Phys. Rev. Lett. **113** (2014) 101101 [astro-ph/1405.5303].
 - [3] M.G. Aartsen et al. (IceCube Collaboration), *Observation of Astrophysical Neutrinos in Four Years of IceCube Data*, PoS(ICRC2015) (2015) 1081 [astro-ph/1510.05223].
 - [4] R. Aloisio, *Ultra High Energy Cosmic Rays and Neutrinos*, [astro-ph/1603.05886].
 - [5] M.G. Aartsen et al. (IceCube Collaboration, Pierre Auger Collaboration and Telescope Array Collaboration), *Search for correlations between the arrival directions of IceCube neutrino events and ultrahigh-energy cosmic rays detected by the Pierre Auger Observatory and the Telescope Array*, JCAP01 (2016) 037 [astro-ph/1511.0948].
 - [6] M. Santander et al. (VERITAS Collaboration and IceCube Collaboration), *Searching for TeV gamma-ray emission associated with IceCube high-energy neutrinos using VERITAS*, PoS(ICRC2015) (2015) 785 [astro-ph/1509.00517].
 - [7] M.G. Aartsen et al. (IceCube Collaboration and LIGO-Virgo Collaboration), *Multimessenger Search for Sources*

- of Gravitational Waves and High-Energy Neutrinos: Results for Initial LIGO-Virgo and IceCube*, Phys. Rev. D **90** (2014) 102002 [astro-ph/1407.1042].
- [8] M.W.E. Smith et al., *The Astrophysical Multimessenger Observatory Network (AMON)*, Astropart. Phys. **45** (2013) 56 [astro-ph/1211.5602].
 - [9] K. Dolag, D. Grasso, V. Springel and I. Tkachev, *Mapping deflections of extragalactic Ultra-High Energy Cosmic Rays in magnetohydrodynamic simulations of the Local Universe*, JETP Lett. **79** (2004) 583 [astro-ph/0310902].
 - [10] G. Sigl, F. Miniati and T. Enßlin, *Ultra-High Energy Cosmic Ray Probes of Large Scale Structure and Magnetic Fields*, Phys. Rev. D **70** (2005) 043007 [astro-ph/0401084].
 - [11] R. Jansson and G.R. Farrar, *A New Model of the Galactic Magnetic Field*, Astrophys. J. **757** (2012) 14 [astro-ph/1204.3662].
 - [12] M.S. Pshirkov, P.G. Tinyakov, P.P. Kronberg and K.J. Newton-McGee, *Deriving global structure of the Galactic Magnetic Field from Faraday Rotation Measures of extragalactic sources*, Astrophys. J. **738** (2011) 192 [astro-ph/1103.0814].
 - [13] R. Jansson and G.R. Farrar, *The Galactic Magnetic Field*, Astrophys. J. **761** (2012) L11 [astro-ph/1210.7820].
 - [14] A. Porcelli et al. (Pierre Auger Collaboration), *Measurements of X_{max} above 10^{17} eV with the fluorescence detector of the Pierre Auger Observatory*, PoS(ICRC2015) (2015) 420.
 - [15] A. Aab et al. (Pierre Auger Collaboration), *Depth of Maximum of Air-Shower Profiles at the Pierre Auger Observatory: Measurements at Energies above $10^{17.8}$ eV*, Phys. Rev. D **90** (2014) 122005 [astro-ph/1409.4809].
 - [16] M.G. Aartsen et al. (IceCube Collaboration), *Evidence for Astrophysical Muon Neutrinos from the Northern Sky with IceCube*, Phys. Rev. Lett. **115** (2015) 081102 [astro-ph/1507.04005].
 - [17] R. Alves Batista et al., *CRPropa: a public framework to propagate UHECRs in the universe*, in *Proceedings of the 33rd International Cosmic Ray Conference*, Rio de Janeiro, Brasil, 2013 [astro-ph/1411.2259].
 - [18] R.C. Gilmore, R.S. Somerville, J.R. Primack and A. Domínguez, *Semi-analytic modeling of the EBL and consequences for extragalactic gamma-ray spectra*, MNRAS **422** (2012) 3189 [astro-ph/1104.0671].
 - [19] S. Mollerach and E. Roulet, *Magnetic diffusion effects on the ultra-high energy cosmic ray spectrum and composition*, JCAP **1310** (2013) 013 [astro-ph/1305.6519].
 - [20] J.A. Carpio and A.M. Gago, *Impact of Galactic magnetic field modeling on searches of point sources via ultrahigh energy cosmic ray -neutrino correlations*, Phys. Rev. D **93** (2016) 023004 [astro-ph/1507.02781].
 - [21] R. Fisher, *Dispersion on a Sphere*, Proc. R. Soc. A **217**, 295 (1953).
 - [22] K.M. Górski et al., *HEALPix: A Framework for High Resolution Discretization and Fast Analysis of Data Distributed on the Sphere*, Astrophys. J. **622** (2005) 759 [astro-ph/0409513].
 - [23] J. Braun et al., *Methods for point source analysis in high energy neutrino telescopes*, Astropart. Phys. **29** (2008) 299 [astro-ph/0801.1604].